

# Optimal Real-Time Operation Strategy for Microgrid: An ADP-Based Stochastic Nonlinear Optimization Approach

Hang Shuai <sup>✉</sup>, *Student Member, IEEE*, Jiakun Fang <sup>✉</sup>, *Member, IEEE*, Xiaomeng Ai <sup>✉</sup>, *Member, IEEE*, Jinyu Wen <sup>✉</sup>, *Member, IEEE*, and Haibo He <sup>✉</sup>, *Fellow, IEEE*

**Abstract**—This paper proposes an approximate dynamic programming (ADP) based algorithm for the real-time operation of the microgrid under uncertainties. First, the optimal operation of the microgrid is formulated as a stochastic mixed-integer nonlinear programming (MINLP) problem, combining the ac power flow and the detailed operational character of the battery. For this NP-hard problem, the proposed ADP based energy management algorithm decomposes the original multitime periods MINLP problem into single-time period nonlinear programming problems. Thus, the sequential decisions can be made by solving Bellman's equation. Historical data is utilized offline to improve the optimality of the real-time decision, and the dependency on the forecast information is reduced. Comparative numerical simulations with several existing methods demonstrate the effectiveness and efficiency of the proposed algorithm.

**Index Terms**—Microgrid, real-time optimization, approximate dynamic programming (ADP), AC power flow, battery.

## NOMENCLATURE

### Parameters

$a_g, b_g, c_g$	The fuel cost coefficients of generator $g$ .
$C_{sup,g}$	The start up cost of generator $g$ .
$c_{bat}$	Per KWh price for the battery.
$D_{i,t}^p, Q_{i,t}^q$	Active and reactive power demand of the node $i$ at time $t$ , respectively.
$E_{max}, E_{min}$	Maximum and minimum state-of-charge of the battery.

Manuscript received September 5, 2017; revised January 12, 2018 and April 10, 2018; accepted July 1, 2018. Date of publication July 11, 2018; date of current version March 21, 2019. This work was supported in part by the National Natural Science Foundation of China under Grant 51529701, and in part by the Fundamental Research Funds for the Central Universities, HUST (2018JYCXJ030). Paper no. TSTE-00815-2017. (*Corresponding author: Xiaomeng Ai.*)

H. Shuai, X. Ai, and J. Wen are with the State Key Laboratory of Advanced Electromagnetic Engineering and Technology, School of Electrical and Electronic Engineering, Huazhong University of Science and Technology, Wuhan 430074, China (e-mail: hang\_shuai@foxmail.com; xiaomengai1986@foxmail.com; jinyu.wen@hust.edu.cn).

J. Fang is with the Department of Energy Technology, Aalborg University, Aalborg DK9220, Denmark (e-mail: jiakun.fang@gmail.com).

H. He is with the Department of Electrical, Computer, and Biomedical Engineering, University of Rhode Island, Kingston, RI 02881 USA (e-mail: haibohe@uri.edu).

Color versions of one or more of the figures in this paper are available online at <http://ieeexplore.ieee.org>.

Digital Object Identifier 10.1109/TSTE.2018.2855039

$G_{ij}, B_{ij}$

$I_{i,m}$

$K$

$N_{node}$

$N_s$

$P^{c,max}, P^{d,max}$

$P_g^{min}, P_g^{max}$

$P_l^{max}$

$R_{up,g}, R_{dn,g}$

$R_{in}$

$T$

$T_{g,on}, T_{g,off}$

$\Delta t$

$V_r, C_r$

$V_{i,t}^{min}, V_{i,t}^{max}$

$W_t^A$

$W_t^F$

$\eta_t^{d,min}, \eta_t^{c,min}$

$\varepsilon_t$

### Variables

$C_t(\cdot)$

$C_{bat,t}$

$C_{bat,t}^l$

$D_{bat,t}^l$

$F_0^*$

Real and imaginary parts of the nodal admittance matrix, respectively.

The element of the node - generator correlation matrix.

Polarisation constant of battery.

Total number of nodes in the microgrid.

Total number of the generators which include controllable generator, uncontrollable generator, and the battery.

Rated charge and discharge power of the battery, respectively.

The minimum/maximum active power output of the controllable generator  $g$ .

Maximum power transmission limitation of lines  $l \in L$ .

Ramp-up and Ramp-down limits of the controllable generator  $g$ .

Internal resistance of the battery.

Optimization horizon.

Minimum on and off time of the controllable generator  $g$ .

Time step.

Rated voltage and rated capacity of the battery respectively.

Minimum/maximum voltage limitations of all nodes, respectively.

Actual value of stochastic variables.

Forecast value of stochastic variables.

Minimum discharge and charge efficiency limit of the battery, respectively.

Forecast error distribution.

Operation cost of the microgrid in time period  $t$ .

Operation cost of the battery in time period  $t$ .

Power consumption of a battery during charge, which equals to the charging loss of the battery.

Power consumption of a battery during discharge, which equals to the discharging loss plus the actual discharging power.

Optimal operation cost of the microgrid.

$P_{bat,t}^d, P_{bat,t}^c$	Discharge and charge power of the battery, respectively.
$P_{g,t}, P_{grid,t}$	Output of the generator $g$ and the power exchange between microgrid and upper level grid at time $t$ .
$P_{l,t}$	Power transmission of the line $l$ at time $t$ .
$P_{s,t}, Q_{s,t}$	Active and reactive power generation of the power source $s$ at time $t$ , respectively. $s$ includes the wind and solar power, MT, DE, battery, and the power grid.
$p_t$	Electricity price of the power market.
$S_{g,t}$	Time of the controllable generator $g$ has been continuously operated or has been stopped until time $t$ .
$S_t, S_t^x$	State variables and post-decision state variables, respectively.
$sd_{g,t}, su_{g,t}$	Shutdown indicator and startup indicator of generator $g$ , respectively.
$s_{g,t}$	On/Off state of the generator $g$ during time period $t$ . $s_{g,t} \in \{0, 1\}$ , where 0 represents the off-line state and 1 represents the online state.
$t$	Time index.
$V_i$	Voltage amplitude of the node $i$ .
$V_t(\cdot)$	Value function.
$\bar{V}_t(\cdot)$	Approximated value function.
$W_t$	Exogenous information.
$x_t$	Decision variables.
$\delta_{i,j,t}$	Phase angle difference between node $i$ and $j$ .
$\eta_t^c, \eta_t^d$	Charge and discharge efficiency of the battery, respectively.

## I. INTRODUCTION

**T**O REDUCE the dependence on fossil fuels and the release of greenhouse gases, renewable energy such as the wind and solar power have been vigorously developed worldwide [1]–[4]. The microgrid, as an effective way to utilize distributed renewable energy takes the advantages of managing the distributed generators (DGs), distributed energy storage (DES), and local demands in a more decentralized way [5]. The energy management of microgrids ensures the optimal coordination between various DGs and electricity loads to provide cost-effective, high-quality and reliable energy. To operate the microgrid more economically and efficiently, the operational optimization research has been widely investigated [5]–[12]. Generally, the existing work can be categorized into the problem formulation and the optimization algorithms.

To formulate the optimization problem for the real-time operation of the microgrid, both the network and the devices need to be modeled. To simplify the problem, network power flow constraints are usually neglected in most of the prior works [5]–[7], [13], [14]. DC power flow is widely adopted in transmission network [15], [16], but it is not suitable for the distribution system level [17]. So for the microgrids, the AC power flow is necessary to properly represent the reactive power requirements, network power losses, node voltage limitations, etc. [17]–[20]. On the other hand, accurate component models are critical to obtaining executive operation strategies. For instance, the nonlinear

model of micro-sources [21] and power electronic devices [14] have been well studied. Energy storage system (ESS) is another essential device in a microgrid, but the relationship between the efficiency of energy conversion and the state-of-charge (SOC) is rather complex [22], [23].

From the mathematical programming point of view, not only the network constraints but also the devices such as energy storages will introduce the nonlinearities to the microgrid optimization. In addition to these nonlinearities, discrete decision variables (e.g., the on/off decisions of dispatchable generators and charge/discharge decisions of the storage) will further make the optimization become a non-convex problem. Consequently, the optimal operation of the microgrid is formulated as mixed-integer nonlinear programming (MINLP) problem.

Mathematically, there is no ultimate solution technique for the MINLP problem [5]. Although MINLP solvers such as CONOPT and BARON are commercialized, they cannot find solutions in reasonable times even for a small-scale system [25]. Some meta-heuristic methods [7]–[10] such as particle swarm optimization (PSO) have been employed, yet the computational burden rises exponentially with the number of variables and constraints. The hierarchical optimization methods [26] are also used, but the global optimality cannot be guaranteed. In addition to nonlinearities, the uncertainties brought by distributed renewable energy and demand side makes the real-time scheduling of the microgrid even more challenging. To cope with the uncertainties, several approaches such as chance constraints method [27], scenario tree method [28], etc. are proposed. When forecast error occurs, the day-ahead scheduling needs to be adjusted [21] during real-time operation. Model predictive control (MPC) is a commonly used real-time optimization method [14], [17], [29] to re-dispatch the flexible regulation devices in the microgrid. However, the historical operational experiences are not fully utilized in the above literature, so the performance of the MPC based algorithms is influenced by the accuracy of intra-day information. With the increasing number of facilities in the microgrid and the system complexity, the scale of the optimization problem raises, hence decomposition techniques are needed to break the large-scale optimization into small subproblems [17]. The hierarchical optimization methods are also used in [26], [42]. The two stage stochastic optimal energy and reserve management is proposed in [30], and the sliding-window based online algorithm is proposed for real-time energy management in [31]. In [32], [33], distributed energy management algorithms, e.g., alternating direction method of multipliers, are applied in the online optimization of microgrid.

To tackle the above-mentioned challenges such as nonlinearities, stochasticities, etc., the approximate dynamic programming (ADP) based energy management algorithm (ADP-EMA) for the real-time operation of the microgrid under uncertainties is proposed in this paper. ADP is a powerful stochastic optimization modeling method. It decomposes a multi-time-period optimization problem into a sequence of time-indexed sub-problems [34]–[39]. These sub-problems are solved successively forward through time over the optimization horizon. Besides, ADP embeds empirical knowledge in the decision process, so the sub-problems are connected by the impact of the

current decision on the future. The proposed algorithm has following advantages.

- 1) the proposed algorithm is capable of decomposing the multi-time-period optimization into the time-indexed sub-problems. Thus the sequential decisions can be made by solving Bellman's equation.
- 2) with the decomposition, the proposed algorithm partially handles the mixed-integer nonlinear programming introduced by practical considerations. The integral variables are removed using the lookup tables following the principles in [39].
- 3) the proposed algorithm can deal with the stochasticity by embedding the empirical knowledge in the historical operational data.
- 4) with the empirical knowledge embedded in the real-time decision process, the proposed algorithm reduces the dependency of optimality on the forecast information.

The contributions of this paper are two-fold. From the modeling perspective, the detailed microgrid optimization model is built, combining the AC power flow constraints and the detailed battery model for the first time. The model can reflect the charge/discharge characteristics and the operation cost of the energy storage device. From algorithmic perspective, the ADP based real-time energy management strategy (i.e., ADP-EMA) for microgrid is proposed.

The remainder of the paper is structured as follows. Section II formulates the battery model. Section III formulates the mathematical model of the microgrid. Then an ADP based stochastic optimization algorithm for the microgrid operation, i.e., ADP-EMA, is proposed in Section IV. Numerical simulations are designed to demonstrate the validity of the proposed ADP-EMA in Section V. Conclusions are summarized in Section VI.

## II. DETAILED BATTERY MODEL

Energy storage device is an important component in microgrids. Currently, the lead-acid battery and lithium battery are most widely utilized energy storage devices, and hence modeled in this work. According to practical experiences, the efficiency of the battery depends on the physical state of battery. Reference [23], [24] developed a novel battery model according to the characteristics of lead-acid and lithium-ion batteries. In the model, the charging and discharging efficiencies are modeled as a nonlinear function of the charging and discharging power and SOC of the battery:

$$D_{bat,t}^l = \frac{10^3 \left( R_{in} + \frac{K}{SOC_t} \right)}{V_r^2} (P_{bat,t}^d)^2 + \left( \frac{10^3 C_r \cdot K (1 - SOC_t)}{SOC_t \cdot V_r^2} + 1 \right) P_{bat,t}^d \quad (1)$$

$$C_{bat,t}^l = \frac{10^3 \left( R_{in} + \frac{K}{1.1 - SOC_t} \right)}{V_r^2} (P_{bat,t}^c)^2 + \frac{10^3 C_r \cdot K (1 - SOC_t)}{SOC_t \cdot V_r^2} P_{bat,t}^c \quad (2)$$

$$\eta_t^d = \frac{P_{bat,t}^d}{D_{bat,t}^l} \quad (3)$$

$$\eta_t^c = 1 - \frac{C_{bat,t}^l}{P_{bat,t}^c} \quad (4)$$

The model proposed in [23] assumes that the maximum charge/discharge power is constant. However, the laboratory and field tests reveal that the charging and discharging power limits of the batteries are related to SOC [22]. Their relationship is established as follows:

$$0 \leq P_{bat,t}^d \leq \min \left\{ P_{bat,t}^{d,\max}(SOC_t, \eta_t^{d,\min}), P_{bat,t}^{d,\max} \right\} \quad (5)$$

$$0 \leq P_{bat,t}^c \leq \min \left\{ P_{bat,t}^{c,\max}(SOC_t, \eta_t^{c,\min}), P_{bat,t}^{c,\max} \right\} \quad (6)$$

From (1)–(4), the discharge efficiency is positively correlated with SOC, while the charge efficiency and SOC are inversely related. The charging and discharging efficiencies decreases with the increase of the power at the same SOC. The right-hand side of (5) and (6) can be calculated by (1)–(4) when  $\eta_t^{d,\min}$  and  $\eta_t^{c,\min}$  are given, which are shown as follows:

$$P_{bat,t}^{d,\max}(SOC_t, \eta_t^{d,\min}) = \frac{V_r^2 SOC_t \left( \frac{1}{\eta_t^{d,\min}} - 1 \right) - 10^3 C_r K (1 - SOC_t)}{10^3 (R_{in} \cdot SOC_t + K)} \quad (7)$$

$$P_{bat,t}^{c,\max}(SOC_t, \eta_t^{c,\min}) = \frac{SOC_t V_r^2 (1 - \eta_t^{c,\min}) - 10^3 C_r K (1 - SOC_t)}{10^3 \cdot SOC_t \left( R_{in} + \frac{K}{1.1 - SOC_t} \right)} \quad (8)$$

The temporal evolution of the SOC can be formulated in a discrete form

$$SOC_t = \begin{cases} SOC_{t-\Delta t} - \frac{D_{bat,t}^l \Delta t}{E_{\max}}, & P_{bat,t}^d > 0 \\ SOC_{t-\Delta t} + \frac{(P_{bat,t}^c - C_{bat,t}^l) \Delta t}{E_{\max}}, & P_{bat,t}^c > 0 \end{cases} \quad (9)$$

It should subject to the min/max capacities

$$\frac{E_{\min}}{C_r} \leq SOC_t \leq \frac{E_{\max}}{C_r} \quad (10)$$

The operational cost of the battery is assumed to be proportional to its charging and discharging power which can be expressed as [23]

$$C_{bat,t} = \begin{cases} c_{bat} D_{bat,t}^l \Delta t, & P_{bat,t}^d > 0 \\ c_{bat} C_{bat,t}^l \Delta t, & P_{bat,t}^c > 0 \end{cases} \quad (11)$$

In addition to the operational characteristics (1)–(11), the output power  $P_{bat,t}$  is calculated by

$$P_{bat,t} = P_{bat,t}^d - P_{bat,t}^c, \forall t \quad (12)$$

The following constraint ensures that the battery cannot be charged and discharged at the same time.

$$P_{bat,t}^d \cdot P_{bat,t}^c = 0, \forall t \quad (13)$$

It can be seen from (1)–(13) that the battery model adopted in this work is rather complex with highly nonlinear relationships between variables and parameters.

### III. MATHEMATICAL MODEL OF THE MICROGRID

In this section, the optimization model for the energy management of the microgrid is established. Only the single microgrid is investigated. The microgrid is composed of dispatchable sources (DS) including micro-gas turbine (MT), diesel generator (DE), battery storage, and non-dispatchable sources (NS) such as wind turbines (WT) and photovoltaic (PV) panel. The optimization problem is to schedule the on/off decision of dispatchable generators (DG) (e.g., MT and DE) in DS, the charge/discharge status of the battery, the power outputs of DS, and the power exchange between the microgrid and the upper-level grid.

#### A. Objective Function

The real-time energy management of microgrid is formulated as a Markov Decision Processes (MDP). The optimization variables includes the state variables and the decision variables [36]. State variables at time  $t$  include SOC of the battery  $SOC_t$ , unit commitment  $s_{g,t}$ , generation dispatch of DG  $P_{g,t}$ , power purchased from electricity market  $P_{grid,t}$ , generation dispatch of NS  $P_{r,t}$ , active load  $D_t$ , reactive load  $Q_t$ , and electricity price  $p_t$ . These variables are aggregated in vector  $S_t$ . The decision variables  $x_t$  include startup indicator  $su_{g,t}$ , shutdown indicator  $sd_{g,t}$  of DG, and the power output of the battery  $P_{bat,t}$ . The objective is to minimize the operation cost of the microgrid over finite optimization horizon  $\Gamma = \{\Delta t, 2\Delta t, \dots, T - \Delta t, T\}$  which can be expressed as

$$F_0^* = \min_{x_{\Delta t}, \dots, x_T} E \left\{ \sum_{t=\Delta t}^T C_t(S_t, x_t) \right\} \quad (14)$$

$$C_t(S_t, x_t) = s_{g,t} (a_g P_{g,t}^2 + b_g P_{g,t} + c_g) \Delta t + C_{sup,g}(s_{g,t} - s_{g,t-\Delta t}) + p_t P_{grid,t} \Delta t + C_{bat,t} \quad (15)$$

where  $E(\cdot)$  represents the expectation.  $s_{g,t}$  is determined by startup indicator  $su_{g,t}$  and shutdown indicator  $sd_{g,t}$ . The first part of (15) represents the fuel cost of DG (e.g., MT and DE) which is a quadratic function of the output power. The startup cost of DG is also considered which is denoted by  $C_{sup,g}$ ; The third part represents the cost related to the power exchange between microgrid and upper-level grid; The operation cost of the battery is represented by the last part of the objective function  $C_{bat,t}$ .

#### B. Constraints

Following constraints are considered in this work.

1) *Power Flow Constraints*: In the microgrid, due to the higher resistance-to-reactance ratio of the power cables, the AC power flow constraints should be adopted in the problem

formulation.

$$\begin{aligned} V_{i,t} & \sum_{j=1}^{N_{node}} V_{j,t} (G_{ij} \cos \delta_{ij,t} + B_{ij} \sin \delta_{ij,t}) \\ & = \sum_{s=1}^{N_s} I_{i,s} P_{s,t} - D_{i,t}^p \quad \forall t \\ V_{i,t} & \sum_{j=1}^{N_{node}} V_{j,t} (G_{ij} \sin \delta_{ij,t} - B_{ij} \cos \delta_{ij,t}) \\ & = \sum_{s=1}^{N_s} I_{i,s} Q_{s,t} - Q_{i,t}^q \quad \forall t \end{aligned} \quad (16)$$

where  $s \in \{WT, PV, MT, DE, battery, grid\}$ ;

2) *Upper and Lower Limits of the Outputs of Dispatchable Generators*:

$$P_g^{\min} s_{g,t} \leq P_{g,t} \leq P_g^{\max} s_{g,t} \quad \forall g, \forall t \quad (17)$$

3) *Ramping Rates of Dispatchable Generators*: For all the generators

$$\begin{aligned} P_{g,t} - P_{g,t-\Delta t} & \leq R_{up,g} \Delta t \cdot s_{g,t-\Delta t} \\ & + P_g^{\min} (s_{g,t} - s_{g,t-\Delta t}) + P_g^{\max} (1 - s_{g,t}) \\ P_{g,t-\Delta t} - P_{g,t} & \leq R_{dn,g} \Delta t \cdot s_{g,t} + P_g^{\min} (s_{g,t-\Delta t} - s_{g,t}) \\ & + P_g^{\max} (1 - s_{g,t-\Delta t}) \end{aligned} \quad (18)$$

4) *Minimum ON/OFF Time Limits of Dispatchable Generators*:

$$\begin{cases} (s_{g,t-\Delta t} - s_{g,t})(S_{g,t-\Delta t} - T_{g,on}) \geq 0 \\ (s_{g,t} - s_{g,t-\Delta t})(-S_{g,t-\Delta t} - T_{g,off}) \geq 0 \end{cases} \quad \forall g, \forall t \quad (19)$$

$S_{g,t}$  is ON (if  $>0$ ) or OFF (if  $<0$ ) time counters of unit  $g$  until time  $t$ .

5) *Voltage Amplitude Constraints*: For all the nodes in the network, the voltage magnitude is bounded by

$$V_{i,t}^{\min} \leq V_{i,t} \leq V_{i,t}^{\max} \quad \forall i, \forall t \quad (20)$$

6) *Power Cable Capacity Constraints*: The power cable capacity constraints are also considered

$$P_{l,t} \leq P_l^{\max} \quad \forall l, \forall t \quad (21)$$

7) *Battery Constraints*: All the constraints are given by (1)–(13).

From above equations, since the uncertainties introduced by renewable energy, electricity price, and demand side, the stochasticity is introduced to the formulated mixed-integer nonlinear programming (MINLP) problem. For this kind of problem, meta-heuristic algorithms, e.g., PSO, and hierarchical optimization method [26] are available methods. However, these optimization algorithms can not ensure the optimality of the solution. Moreover, the algorithms are seldom applied in



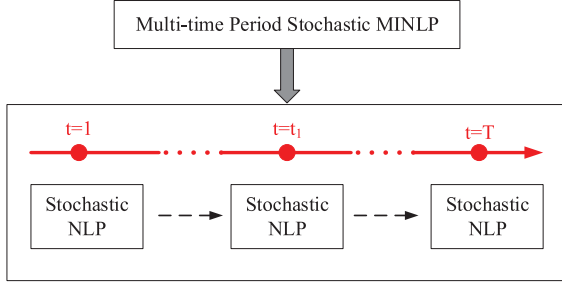


Fig. 1. Decomposition of MINLP optimization using ADP.

real-time optimization process. This paper proposed to use ADP algorithm to solve this stochastic MINLP problem and obtain the real-time operation strategy simultaneously. The following part sets up the process of using ADP to solve the problem.

#### IV. APPROXIMATE DYNAMIC PROGRAMMING BASED ENERGY MANAGEMENT ALGORITHM

ADP is an effective method to solve MDP problem. Using this approach, the original multi-time period stochastic MINLP optimization can be decomposed into several single-period NLP sub-problems, as shown in the Fig. 1. This time-dependent decomposition method reduces the difficulty of solving the original problem. Before the presenting of the proposed real-time energy management algorithm, we first define the state variables, decision variables, exogenous information, and transition function which are basic elements to MDP [39].

##### A. Definition of Basic Elements

1) *State Variables & Decision Variables*: According to Section III-A, the state variables can be defined as

$$S_t = \{SOC_t, s_{g,t}, P_{g,t}, P_{grid,t}, P_{pv,t}, P_{wt,t}, D_t, Q_t, p_t\} \quad (22)$$

The exogenous information at time  $t$  is

$$W_t = \{\hat{P}_{pv,t}, \hat{P}_{wt,t}, \hat{D}_t, \hat{Q}_t, \hat{p}_t\} \quad (23)$$

where  $W_t$  represents the information that first arrives between  $t - \Delta t$  and  $t$ .  $\hat{P}_{pv,t}$  is the change in the PV power between forecast value and actual one. Similarly for the other elements in  $W_t$ .

The decision variables of the problem can be defined by

$$x_t = \{su_{g,t}, sd_{g,t}, P_{bat,t}\} \quad (24)$$

2) *Transition Function*: The transition function  $S_{t+\Delta t} = S^M(S_t, x_t, W_{t+\Delta t})$  can map the current state  $S_t$  to the next state  $S_{t+\Delta t}$  according to the decision  $x_t$  and the exogenous information  $W_{t+\Delta t}$ . The SOC transition function is shown in equation (9). The ON/OFF state transition function of DG is given by

$$s_{g,t+\Delta t} = \begin{cases} 1, & \text{if } su_{g,t} = 1, sd_{g,t} = 0 \\ 0, & \text{if } su_{g,t} = 0, sd_{g,t} = 1 \end{cases} \quad (25)$$

The transition of other elements in  $S_t$  can be calculated by:

$$W_{t+\Delta t}^A = W_{t+\Delta t}^F + W_{t+\Delta t} \quad (26)$$

where  $W_{t+\Delta t}^A = \{P_{pv,t+\Delta t}, P_{wt,t+\Delta t}, D_{t+\Delta t}, Q_{t+\Delta t}, p_{t+\Delta t}\}$  and  $W_{t+\Delta t}^F = \{P_{pv,t+\Delta t}^F, P_{wt,t+\Delta t}^F, D_{t+\Delta t}^F, Q_{t+\Delta t}^F, p_{t+\Delta t}^F\}$ .

##### B. ADP Based Optimization Approach

1) *Lookup Tables Approximation*: According to MDP theory, the stochastic optimization problem of the form (14) can be reformulated as the MDP problem and solved recursively using the Bellman's equation (27).

$$V_t(S_t) = \min_{x_t} \{C_t(S_t, x_t) + E(V_{t+\Delta t}(S_{t+\Delta t})|S_t)\} \quad (27)$$

$$V_{t+\Delta t}(S_{t+\Delta t}) = \sum_{\tau=t+\Delta t}^T \{C_\tau(S_\tau, x_\tau)\} \quad (28)$$

$V_{t+\Delta t}(S_{t+\Delta t})$  is the value function which represents the operation cost from  $t + \Delta t$  to  $T$  when system start from state  $S_{t+\Delta t}$ . *Dynamic programming* (DP) algorithm is a basic algorithm to solve the MDP problem by backward through time. DP solves (27) from the last period  $t = T$  to the first one  $t = \Delta t$  to get the optimal value function  $V_t(S_t)$  ( $t \in \Gamma$ ). Then we solve the Bellman's equation forward through time to obtain the optimal solution. However, DP will encounter "the curse of dimensionality" due to computing the expectation value in (27) is computationally intractable [39].

ADP is an algorithmic strategy that steps *forward* through time which enables it to solve a variety of multi-time period optimization problems. One of its basic ideas is to use approximated value functions which are updated iteratively in the training process to avoid computing the optimal value function in DP. There are plenty of methods to approximate value functions, for example, parametric representations [34], nonparametric representations [37], [40], [41], and lookup tables [42]. Lookup tables are basic yet a effective way to approximate value function, and it is adopted in this paper. The details of the lookup tables approximation are presented as follows.

To overcome the curse of dimensionality in information space,  $W_t$ , the post-decision formulation of Bellman's equation is formulated as follows

$$V_t(S_t) = \min_{x_t} \{C_t(S_t, x_t) + V_t^x(S_t^x)\} \quad (29)$$

where  $S_t^x$  is the post-decision state [39] which represents the system state after the decision  $x_t$  has been made but before the new information  $W_{t+\Delta t}$  has arrived.  $V_t^x(S_t^x)$  is the post-decision value function. It represents the operation cost from time  $t + \Delta t$  to  $T$  when the system being in state  $S_t^x$ . From (27) and (29), the relationship between post-decision value function and the expectation of value function is shown as

$$V_t^x(S_t^x) = E(V_{t+\Delta t}(S_{t+\Delta t})|S_t) \quad (30)$$

The expectation in (29) is eliminated by introducing the post-decision value function. But the function  $V_t^x(S_t^x)$  is not known in prior. In this work, we use value tables to approximate

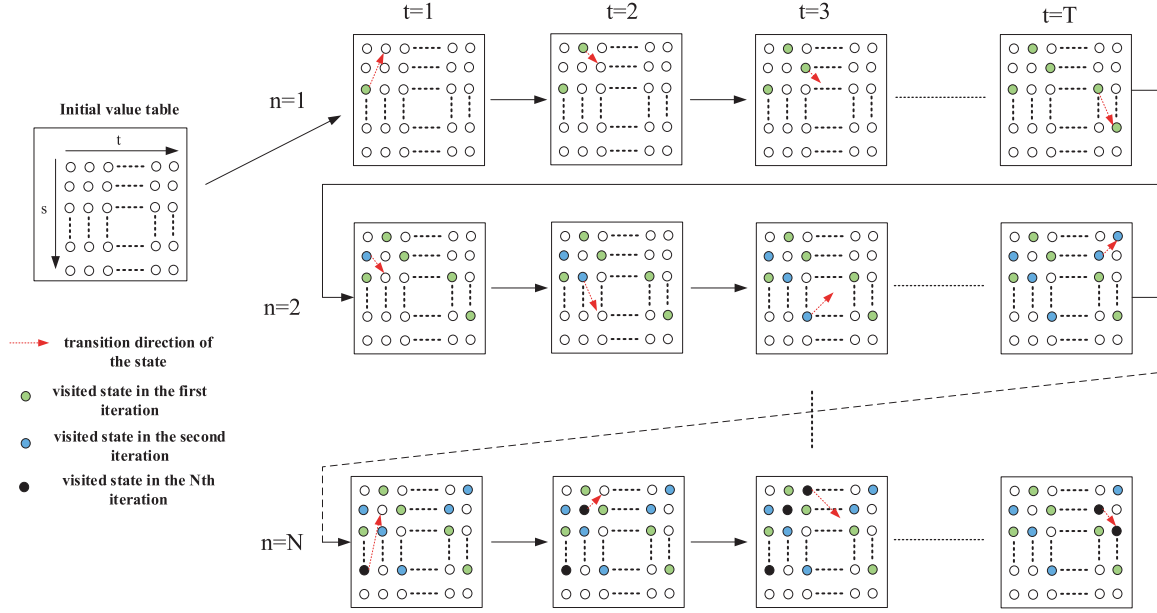


Fig. 2. The value function updating process of the value table.

this function. The approximated value function is denoted by  $\bar{V}_t^x(S_t^x)$ .

The value table establishes the mapping between the discrete system variables and the future operating costs of the system. First, we discretize the state variables and decision variables, as shown in (31).  $G$  represents the elements in  $S_t$  and  $x_t$ .  $d_G$  is the mesh size of variable  $G$ .

$$\Delta G = \frac{G_{\max} - G_{\min}}{d_G} \quad (31)$$

To reduce the size of the state space and decision space, we set the mesh size of the continuous variables in  $S_t$  and  $x_t$  to be 1, except  $SOC_t$  and  $P_{bat,t}$ . In this work, the discrete variables in  $S_t$  are the ON/OFF state of MT and DE. So, the size of the state space  $S_t$  is  $M = 2^2 \cdot d_{SOC}$ . The size of the value table is  $M \times T$ .

2) *Value-table Updating Method*: The value table is updated in each iteration to obtain the optimal solution. At anytime  $t$  and iteration  $n$ , ADP is recursively computing the sample realization of the value of being in the state  $S_t^n$  using the approximated value function obtained in the previous iteration

$$\hat{v}_t^n = \min_{x_t^n} \left\{ C_t(S_t^n, x_t^n) + \bar{V}_t^{x,n-1}(S_t^{x,n}) \right\} \quad (32)$$

where  $\hat{v}_t^n$  is a Monte Carlo (MC) estimate of the value being in the state  $S_t^n$ ;  $n$  indicate the variable in the  $n$ th iteration. Then the value table can be updated according to

$$\bar{V}_{t-\Delta t}^{x,n}(S_{t-\Delta t}^{x,n}) = (1 - \alpha^n) \bar{V}_{t-\Delta t}^{x,n-1}(S_{t-\Delta t}^{x,n}) + \alpha^n \hat{v}_t^n \quad (33)$$

where  $\alpha^n$  is the stepsize, and  $\alpha^n \in (0, 1)$ . Note that we just update the value respected to the state,  $S_{t-\Delta t}^{x,n}$ , we visited in the iteration for every time step. The value function updating process is shown in Fig. 2.

ADP proceeds by estimating the approximation function  $\bar{V}_t^x(S_t^x)$  iteratively. In every time step  $t$ , it needs to traverse all

feasible decisions  $x_t \in X_t$  and find optimal decision by solving (32).  $X_t$  is the feasible decision space which is determined according to the constraints (1)–(10), (19), and (12)–(13). For a feasible decision  $x_t$ , it just indicates the on/off decisions of the dispatchable units and the charge/discharge power of the battery. The output power of all dispatchable units and the power exchange between microgrid and power grid are still unknown. These variables are determined by economic dispatch (ED) algorithm using interior point method. The goal of the ED is to minimize the operation cost  $C_t(S_t, x_t)$  in (11) under the constraints (16)–(18) and (20)–(21). Substitute all the operation cost  $C_t(S_t^n, x_t^n)$  respect to all the decision  $x_t^n$  in (32) to obtain the optimal decision and  $\hat{v}_t^n$ . Then, using (33) to update the element  $\bar{V}_t^x(S_t^x)$  in the value table.

### C. Training Process of the ADP-EMA

The iteration process of the ADP-EMA is shown in Fig. 3. From the figure, the original MINLP problem is decomposed into  $T$  NLP sub-problems. For every feasible decision  $x_t$ , we solve the ED problem to obtain the operation cost  $C_t(S_t, x_t)$ . However, the ED problem is a nonlinear programming problem (without integer variables) solving which is time-consuming. If in each iteration and each period, ED problem is solved for every feasible decision. This will take much time until the algorithm reaches convergence. But note that for the same state variable  $S_t$  and decision variable  $x_t$ , the operation cost  $C_t(S_t, x_t)$  is deterministic. If the exogenous information is deterministic, there is no any uncertainty in the state transition process. Thus, when the ADP algorithm is used to solve the deterministic MINLP problem, to speed up the convergence rate, we establish a one-period contribution function table which is used to store the  $C_t(S_t, x_t)$  corresponding every state-decision pair  $(S_t, x_t)$ . So, in the following iteration, we will not need to solve ED problem if the  $(S_t, x_t)$  pair has occurred in the previous iterations. For

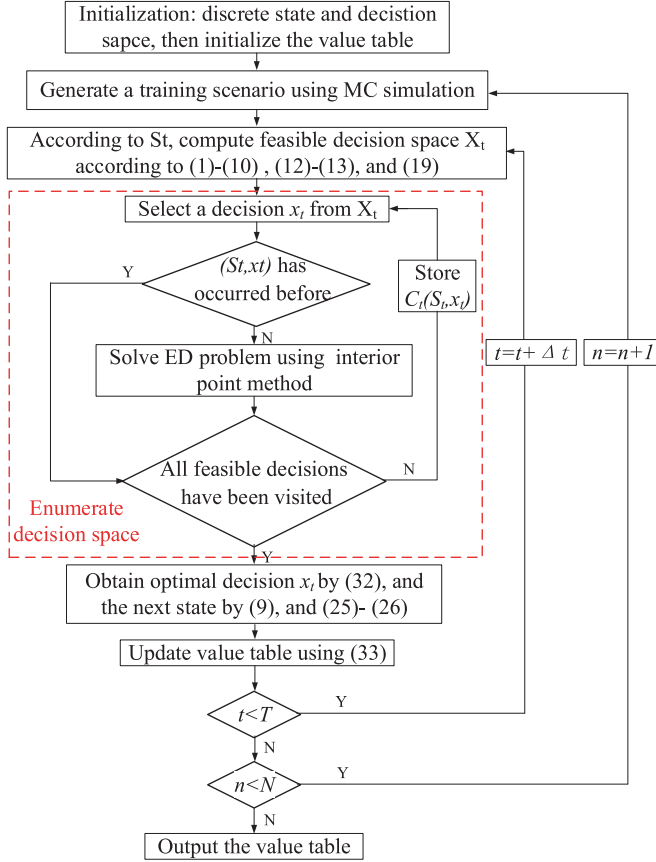


Fig. 3. Training process of the ADP-EMA.

the stochastic case, as the system state  $S_t^n$  is different in different iteration  $n$ , so the above one-period contribution function table will not speed up the convergence rate.

#### D. Real-Time Operation Strategy

The goal of the real-time optimization is to find the optimal decisions under the operation strategy  $\pi$ . In ADP decision framework, the strategy is defined as a function that determines a decision given the available information in state  $S_t$ . After sufficient training, value table can be obtained and then used in real-time decision as follows:

$$X_t^{ADP-EMA}(S_t) = \arg \min_{x_t} \{C_t(S_t, x_t) + \bar{V}_t^{x,N}(S_t^x)\} \quad (34)$$

It is worth to note that  $\bar{V}_t^{x,N}(S_t^x)$  is the final approximated value function in the training process. As shown in Fig. 4, by stepping forward through time, we can obtain the ADP-EMA based optimal operation strategy of the system. The online decision process just use the current state information and the approximated value function.

MPC and myopic policy are another two kinds of commonly used real-time energy management policy. MPC method solves the optimization problem over time horizon  $H$  ( $H < T$ ) at every time step  $t$  using the near future forecast information, while only the decision of current time  $t$  is implemented. Then we repeat the optimization process at the next time  $t + \Delta t$  using the newly

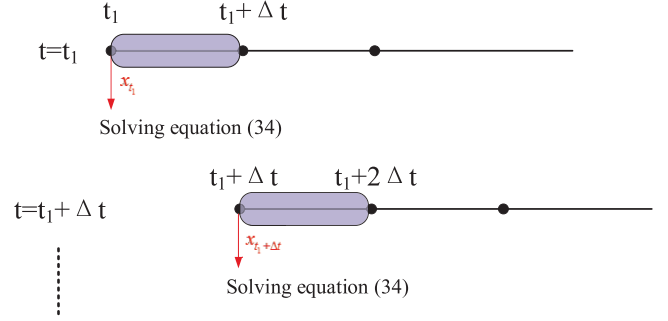


Fig. 4. ADP based real-time decision process.

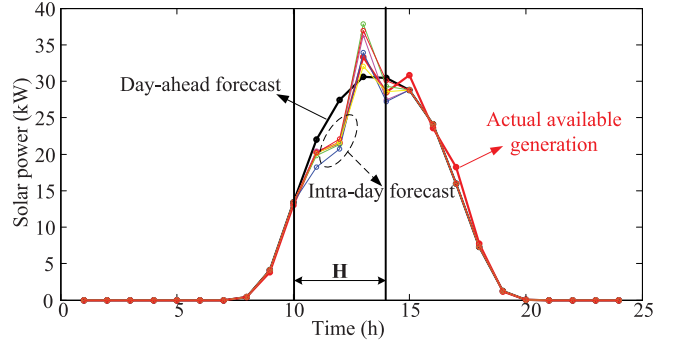


Fig. 5. MPC based real-time decision process.

arrived forecast information. The real-time decision process of MPC can be described using Fig. 5. For instance, in time  $t = 10$  we can obtain the updated PV power forecast from  $t = 11$  to  $t = 14$ . In the figure, we show 5 intra-day forecast scenarios. The real-time operation decision of MPC at time  $t = 10$  can be obtained by solving (35). Similarly, in time  $t = 11$  we get the actual system information of current time and the updated forecast from  $t = 12$  to  $t = 15$ , then the optimal decision  $x_{t=11}$  can be calculated. The MPC based real-time optimization policy is shown as,

$$X_t^{MPC}(S_t) = \arg \min_{x_t, x_{t+\Delta t}, \dots, x_{t+H}} \sum_{t'=t}^{t+H} C_{t'}(S_{t'}, x_{t'}) \quad (35)$$

The myopic policy does not use any forecast information in the optimization. For the classical myopic policy (without tunable parameters), the impact of the current decisions on the future is ignored [39]. The myopic policy based real-time optimization is shown as,

$$X_t^{Myopic}(S_t) = \arg \min_{x_t} C_t(S_t, x_t) \quad (36)$$

To evaluate the performance of the real-time operation strategy, the optimization error  $e_\pi^n$  for scenario  $n$  using operation strategy  $\pi$  can be calculated by

$$e_\pi^n = \frac{F_\pi^n - F_B^n}{F_B^n} \quad (37)$$

Here  $F_\pi^n$  and  $F_B^n$  are the objective function obtained from real-time energy management strategy  $\pi$  and the baseline solution for the  $n$ th scenario, respectively.

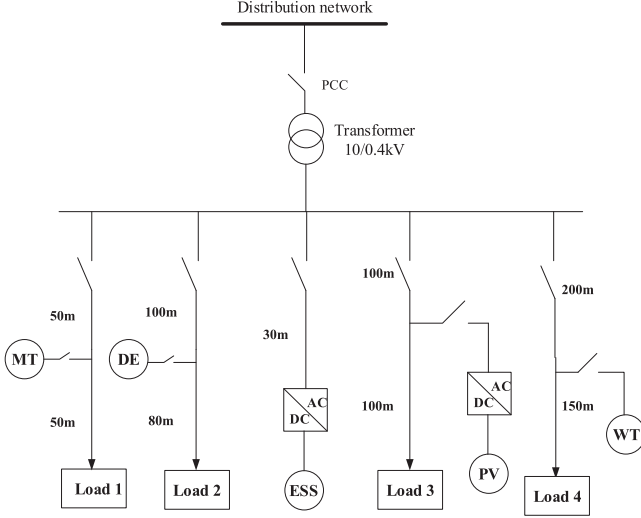


Fig. 6. The schematic diagram of the microgrid.

TABLE I  
PARAMETERS OF THE MT AND DE

Generators	$P_{max}$ (kW)	$P_{min}$ (kW)	$c_m^{SU}$ (\$)	$T_{on}^{min}$ (h)	$T_{off}^{min}$ (h)
MT	30	10	2	1	1
DE	30	10	3	1	1

TABLE II  
THE FUEL COST COEFFICIENTS OF MT AND DE

Generators	$a$ (\$/(kW) <sup>2</sup> h)	$b$ (\$/kWh)	$c$ (\$)
MT	0.00051	0.0397	0.4
DE	0.00104	0.0304	1.3

TABLE III  
PARAMETERS OF THE BATTERY

Item	$E_{max}$ (kWh)	$E_{min}$ (kWh)	$P_{b,max}$ (kW)	$P_{b,min}$ (kW)	$c_{bat}$ (\$/kWh)	$V_r$ (V)
Value	60	18	12	0	0.059	60

## V. NUMERICAL ANALYSIS

In this section, the performance of the ADP-EMA algorithm is examined by numerical experiments on a microgrid benchmark. The schematic diagram is shown in Fig. 6. The microgrid includes dispatchable generators, i.e., MT, DE, the non-dispatchable generators i.e., PV, WT, and a battery. The length of the power cables between all nodes is shown in Fig. 6. For brevity, the types of all the cables are set to be the same. The cable parameters are  $R = 0.64 \Omega/\text{km}$ ,  $X = 0.1 \Omega/\text{km}$ . The parameters of the dispatchable generators and battery are provided from Table I to Table III. For all the simulations below, the SOC and the charge/discharge power of the battery are uniformly discretized into 12 states and 14 states, respectively, i.e.  $d_{SOC} = 12$  and  $d_{P_{bat}} = 14$ . The power factor of all loads in the microgrid is the same and is set to be 0.9. The optimization horizon of all simulations is set to be 24 h, and we set  $\Delta t = 1$  h. All case studies have been run using Matlab 2012 on a 64-bit windows based computer with 4 GB of RAM and Intel Core i5 processor clocking at 2.7 GHz.

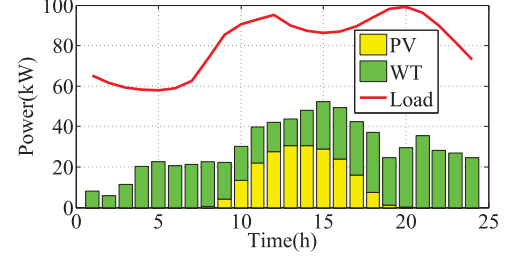


Fig. 7. The power from PV, WT, and the load demand.

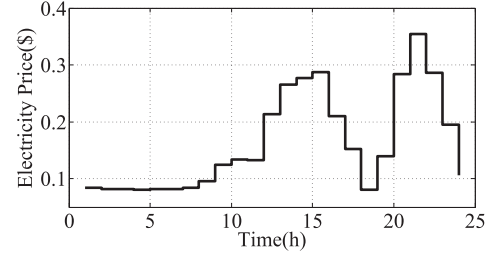


Fig. 8. The electricity price of the power market.

TABLE IV  
THE OPTIMIZATION RESULT OF THE DETERMINISTIC CASE

Algorithm	Cost (\$)	Iteration Number	Computation Time (s)
Myopic	102.68	-	9.26
PSO	95.68	80	208.53
ADP-EMA	90.26	1200	66.4
DP	89.49	-	1595.9

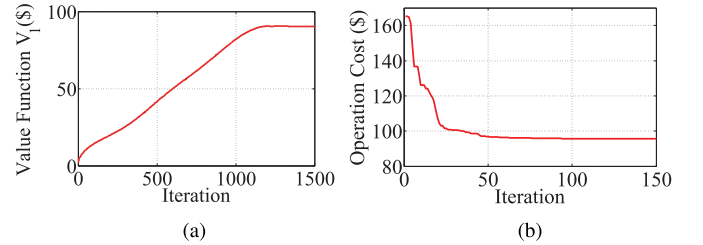


Fig. 9. The convergence process of (a) the ADP-EMA algorithm, (b) the PSO algorithm.

### A. Algorithm Validation in Deterministic Case

For the deterministic case, we need to solve a MINLP problem. The forecast information of the power generation of PV, WT, and the total active load demand is shown in Fig. 7. The electricity price of the power market is shown in Fig. 8.

1) *Algorithm Validity Simulation*: DP and PSO are commonly used methods to solve NP hard problem. To illustrate the validity of the ADP-EMA algorithm, the optimization result of ADP-EMA is compared with PSO algorithm [43], myopic policy, and DP method. The parameter setting of the PSO is as follow. The initial swarm population is 25. The maximum iteration number is 150. The position updating equation of the swarm is the same with [43]. The optimization results of the algorithms are listed in Table. IV and Fig. 9. It can be found that the ADP-EMA algorithm converges in about 1200 iterations. Furthermore, it is observed that ADP-EMA takes less



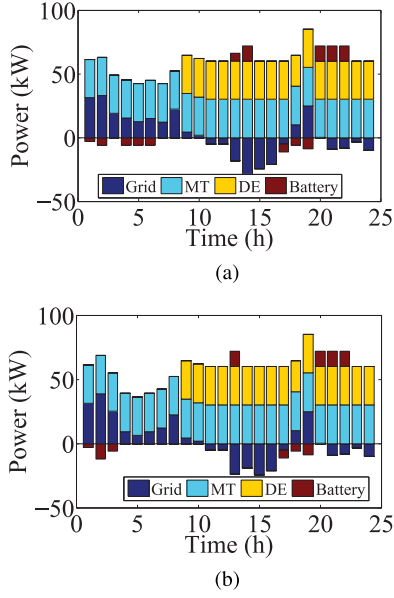


Fig. 10. (a) The output power of all sources for Case 1. (b) The output power of all sources for Case 2.

computational time than PSO and obtained a better solution. Comparing DP and ADP-EMA, the former can obtain global optimality by precisely solving Bellman's equation. The later, on the contrary, can obtain near optimal solution using approximated value functions. But the computational efficiency of DP is not as computationally efficient as ADP. From the simulation result, ADP-EMA solution to be within 0.86% of optimal and the algorithm using much less computational time compared with DP. Finally, myopic policy performs worst among all these algorithms. This result is expected since myopic policy cannot consider the influence of current decision on the future which means it is not a global optimization algorithm.

2) *Comparison Study of the Different Battery Models:* To compare the optimization results of different battery models, two cases are designed. In Case 1, the charge/discharge power limits of the battery is set to be the constant value. In Case 2, the charge/discharge power limits are the function of SOC. The maximum charge/discharge power can be calculated by (8)–(9).

For the two cases, the simulation results are shown in Fig. 10–Fig. 11. From Fig. 10, the MT is always on line as the fuel cost of MT is lower than other sources. During time 0 h–9 h DE is turned off, as the electricity price in power market is below 0.1\$/kWh which cheaper than DE generation. From Fig. 11 (a), it is observed that the battery stores energy in midnight when the electricity price is low, then discharges when the load demand is high in period 12h–13h, and charges again before the peak hour 21h. Lastly, the energy in the battery is discharged to the lower bound in order to store energy in midnight. From the figure, it is observed that the operating SOC window of Case 2 is narrower compared to Case 1 as a result of the variable power limits of the battery. The simulation result is consistent with the conclusion in [22]. The charge/discharge power losses of the battery in the two cases are shown in Fig. 11 (b). The total power losses of the battery in Case 1 and Case 2 are 5.468 kWh and 5.375 kWh, respectively. Besides, the operation cost in Case 2 is higher than

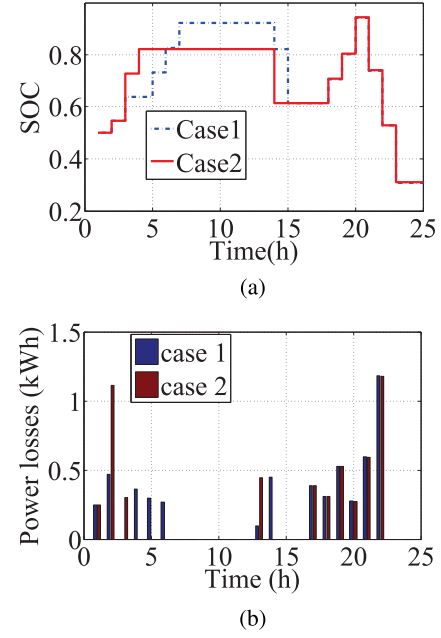


Fig. 11. (a) The SOC of the battery. (b) The charge/discharge efficiency of the battery.

TABLE V  
PERCENTAGE OF OPTIMALITY FOR DECISIONS GENERATED FROM THE ADP-EMA

Batch index ( $m$ )	10	20	30	40	50	60
Percentage of Optimality (%)	60.48	75.87	83.75	92.60	92.61	98.23

the Case 1 since the variable power limits of charge/discharge process decreased the arbitrage ability of the battery.

### B. Off-Line Training & Real-Time Optimization

1) *Off-Line Training:* To demonstrate that the ADP-EMA can address the uncertainties, the following stochastic cases are designed. Assume that the day-ahead forecast error of the wind power  $\varepsilon_t^w$ , solar power  $\varepsilon_t^{pv}$ , electricity price  $\varepsilon_t^p$ , and load  $\varepsilon_t^{load}$  obey Gaussian distribution. Let  $\varepsilon_t^w \sim N(0, 0.1^2)$ , which means the standard deviation of the wind power forecast error is set to be 10 % of its mean value. Similarly, let  $\varepsilon_t^{pv} \sim N(0, 0.1^2)$ ,  $\varepsilon_t^{load} \sim N(0, 0.05^2)$ ,  $\varepsilon_t^p \sim N(0, 0.05^2)$ . Based on these statistics, 1200 historical scenarios are generated using MC simulation and shown in Fig. 12.

Then these 1200 scenarios are divided into 60 groups for the batch training. The average optimization error of ADP-EMA is given by:

$$ERR^m = \frac{1}{N_{batch}} \sum_{n=1}^{N_{batch}} e_{ADP-EMA}^n \quad (38)$$

$ERR^m$  indicates the average deviation of the ADP-EMA solution to the baseline solution for the  $m$ th batch.  $N_{batch}$  is the total scenario number in each batch. We set  $N_{batch} = 20$ .  $e_{ADP-EMA}^n$  represents the optimization error of ADP-EMA for the  $n$ th scenario which can be calculated by (37). The convergence process of the algorithm is illustrated in Table V. After

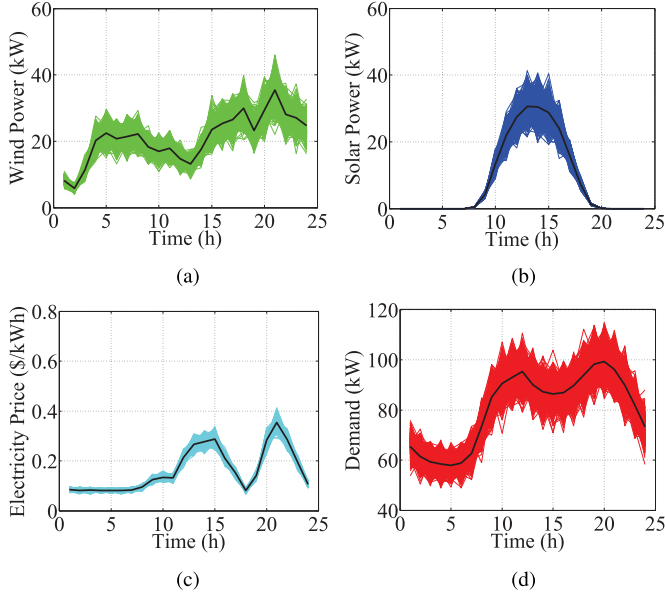


Fig. 12. (a) The sampled wind power scenarios. (b) The sampled solar power scenarios. (c) The sampled electricity price scenarios. (d) The sampled demand scenarios.

TABLE VI  
THE OPTIMIZED OPERATION COST UNDER DIFFERENT ZINTRA-DAY  
FORECAST SCENARIOS USING MPC

Intra-day Forecast Scenario	1	2	3	4	5
Cost (\$)	104.09	104.05	103.07	103.52	102.83
Intra-day Forecast Scenario	6	7	8	9	10
Cost (\$)	104.06	104.11	103.89	102.94	104.53

60 batches of training, the algorithm can reach 98.23% optimality. This means the proposed algorithm is effective to solve the stochastic MINLP problem.

2) *Real-Time Optimization*: After the off-line training with the 1200 scenarios in day-ahead, in the following cases, the well-trained value table will be tested to demonstrate the real-time optimization ability of the ADP-EMA.

The intra-day updated forecast generally more accurate than day-ahead value. In the simulation we assume all the intra-day forecast error obey Gaussian distribution and let  $\varepsilon_t^w \sim N(0, 0.05^2)$ ,  $\varepsilon_t^{pv} \sim N(0, 0.05^2)$ ,  $\varepsilon_t^{load} \sim N(0, 0.02^2)$ ,  $\varepsilon_t^p \sim N(0, 0.03^2)$ . The future forecast information in the following  $H = 4$  hours are updated at each time step. Firstly, we will compare the performances of ADP-EMA and MPC algorithm in real-time optimization. As the problem is MINLP problem, we nested PSO in the MPC optimization process. Under different intra-day forecast scenarios, the optimized operation costs are different. We picked 10 scenarios and the corresponding results are listed in Table. VI. It is worth noting that the actual solar generation curve, wind generation curve, electricity price curve, and load curve are all the same for the 10 scenarios. The only differences between the scenarios are the near-future forecast information. It is observed from the result that the performance of the MPC method is affected by the updated forecast. While ADP successively solves Bellman's equation to get the optimal decision of each time and it reduces the dependency on future

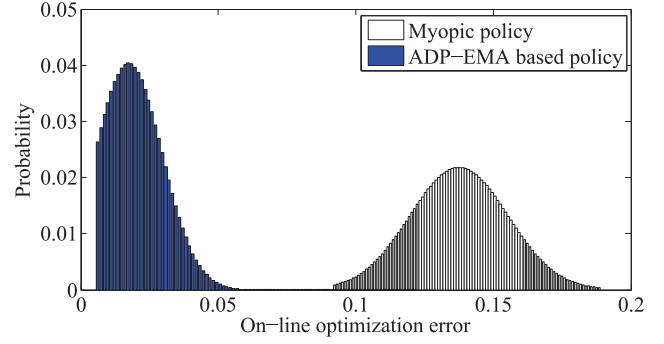


Fig. 13. Real-Time optimization error of ADP-EMA and myopic policy.

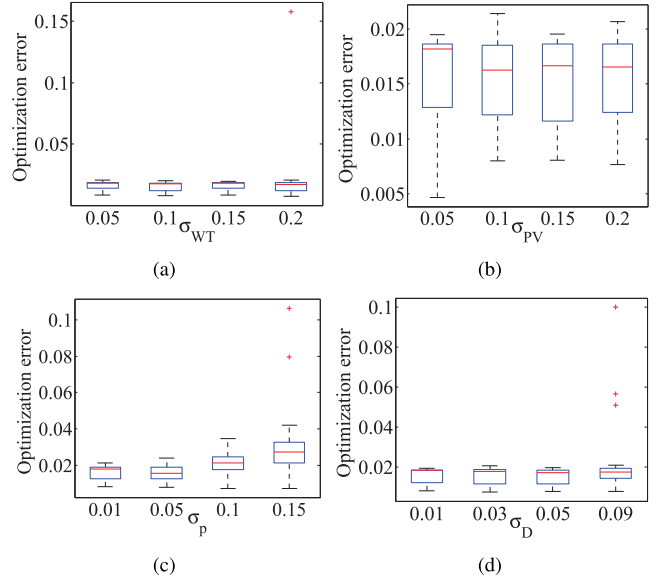


Fig. 14. Optimization error of ADP-EMA corresponding to (a) wind power uncertainty, (b) pv power uncertainty, (c) electricity price uncertainty, (d) demand uncertainty.

forecast information. So the intra-day forecast scenarios will not affect the performance of ADP. Using the proposed ADP-EMA method, the optimization cost of the microgrid is 97.17 \$. We can find that ADP-EMA outperforms MPC. This is because MPC just lookahead  $H$  hours, so the local optimal solutions are obtained. However, the approximated value table enables ADP-EMA can evaluate the influence of the current decisions on all the following periods. So ADP-EMA can obtain a better solution.

From the above simulation results, it can be found that ADP-EMA is not affected by intra-day forecast errors. The myopic policy is a commonly used real-time optimization method which also does not need future forecast information. In the following simulation, we use myopic policy to optimize microgrid operation and compare its performance with ADP-EMA. MC method is adopted to simulate 200 sets of test scenarios according to the day-ahead forecast and the forecast error distribution information. We assume the forecast error of the test data obeys the same distribution as the training data. The real-time optimization results of the two algorithms are shown in Fig. 13. From the result, the average optimization error of the ADP-EMA and myopic policy are 1.80% and 13.75%, respectively. It is

observed that ADP-EMA obtains better performance in real-time decision process compared with myopic policy.

3) *Robustness of the ADP-EMA*: When the day-ahead forecast error distribution of the test scenarios are different from the training scenarios, the real-time optimization performance of the algorithm may be different. To demonstrate ADP-EMA is robust to the wind power prediction error, we set the standard deviation of the wind power forecast  $\sigma_{WT}$  increases from 0.05 to 0.20. The simulation result is shown in Fig. 14(a). The similar simulations are also conducted for PV, electricity demand, and electricity price which are shown in 14(b)–(d). It can be found that the real-time operation strategy is robust to these uncertainties. The average optimization error is always below 3%.

## VI. CONCLUSION

This paper proposes the lookup tables based ADP algorithm for the real-time energy management of the microgrid under uncertainties. The AC power flow constraints and the detailed battery model are considered in the operational model. The detailed battery model proposed in this paper builds the relationship between the SOC and the min/max charge/discharge power limits. For the formulated MINLP optimization problem, we propose an ADP based energy management algorithm. The simulation results demonstrate the effectiveness of the proposed ADP-EMA. Comparative studies with myopic algorithm and model predictive control validate the applicability of the proposed ADP-EMA in real-time decision process with reduced dependency on forecast information. The proposed algorithm is promising to provide a new framework for the real-time energy management of the microgrid. In the future work, the proposed algorithm will be applied in the optimization of multiple microgrids.

## REFERENCES

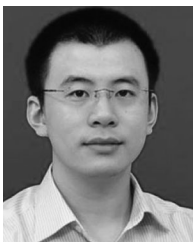
- [1] B. Obama, "The irreversible momentum of clean energy," *Science*, vol. 355, no. 6321, pp. 126–129, Jan. 2017.
- [2] A. Izadian, N. Girrens, and P. Khayyer, "Renewable energy policies: A brief review of the latest U.S. and E.U. policies," *IEEE Ind. Electron. Mag.*, vol. 7, no. 3, pp. 21–34, Sep. 2013.
- [3] C. O'Dwyer, L. Ryan, and D. Flynn, "Efficient large-scale energy storage dispatch: Challenges in future high renewables systems," *IEEE Trans. Power Syst.*, vol. 32, no. 5, pp. 3439–3450, Sep. 2017.
- [4] W. Su and Q. Wang, "Energy management systems in microgrid operations," *Elect. J.*, vol. 25, no. 8, pp. 45–60, 2012.
- [5] A. Parisio, E. Rikos, and L. Glielmo, "A model predictive control approach to microgrid operation optimization," *IEEE Trans. Control Syst. Technol.*, vol. 22, no. 5, pp. 1813–1827, Sep. 2014.
- [6] X. Liu, M. Ding, P. Han, and Y. Peng, "Dynamic economic dispatch for microgrids including battery energy storage," in *Proc. 2nd IEEE Int. Power Electron. Distrib. Gener. Syst. Symp.*, 2010, pp. 914–917.
- [7] Z. J. Bao, Q. Zhou, Z. H. Yang, Q. Z. Xu, and T. Wu, "A multi time-scale and multi energy-type coordinated microgrid scheduling solution-part II: Optimization algorithm and case studies," *IEEE Trans. Power Syst.*, vol. 30, no. 5, pp. 2267–2277, Sep. 2015.
- [8] A. I. Selvakumar and K. Thanushkodi, "A new particle swarm optimization solution to nonconvex economic dispatch problems," *IEEE Trans. Power Syst.*, vol. 22, no. 1, pp. 42–51, Feb. 2007.
- [9] A. Karthikeyan, K. Manikandan, and P. Somasundaram, "Economic dispatch of microgrid with smart energy storage systems using particle swarm optimization," in *Proc. Int. Conf. Comput. Power, Energy Inf. Commun.*, 2016, pp. 783–789.
- [10] V. Mohan, J. G. Singh, and W. Ongsakul, "Sortino ratio based portfolio optimization considering EVs and renewable energy in microgrid power market," *IEEE Trans. Sustain. Energy*, vol. 8, no. 1, pp. 219–229, Jan. 2017.
- [11] F. G. Torres and C. Bordons, "Optimal economical schedule of hydrogen-based microgrids with hybrid storage using model predictive control," *IEEE Trans. Ind. Electron.*, vol. 62, no. 8, pp. 5195–5207, Aug. 2015.
- [12] L. Xu *et al.*, "A co-ordinated dispatch model for electricity and heat in a microgrid via particle swarm optimization," *IEEE Trans. Inst. Meas. Control*, vol. 35, no. 1, pp. 44–55, Feb. 2013.
- [13] P. G. Tian, X. Xiao, K. Wang, and R. X. Ding, "A hierarchical energy management system based on hierarchical optimization for microgrid community economic operation," *IEEE Trans. Smart Grid*, vol. 7, no. 5, pp. 2230–2241, Sep. 2016.
- [14] J. Sachs and O. Sawodny, "A two-stage model predictive control strategy for economic diesel-pv-battery island microgrid operation in rural areas," *IEEE Trans. Sustain. Energy*, vol. 7, no. 3, pp. 903–913, Jul. 2016.
- [15] L. Wu and M. Shahidehpour, "Accelerating Benders decomposition for network-constrained unit commitment problems," *Energy Syst.*, vol. 1, no. 3, pp. 339–376, 2010.
- [16] M. J. Feizollahi, M. Costley, S. Ahmed, and S. Grijalva, "Large-scale decentralized unit commitment," *Electr. Power Energy Syst.*, vol. 73, pp. 97–106, 2015.
- [17] D. E. Olivares, C. A. Canizares, and M. Kazerani, "A centralized energy management system for isolated microgrids," *IEEE Trans. Smart Grid*, vol. 5, no. 4, pp. 1864–1875, Jul. 2014.
- [18] M. Dolan, E. Davidson, I. Kockar, G. Ault, and S. McArthur, "Distribution power flow management utilizing an online optimal power flow technique," *IEEE Trans. Power Syst.*, vol. 27, no. 2, pp. 790–799, May 2012.
- [19] M. Pirnia, C. A. Caniñares, K. Bhattacharya, and A. Vaccaro, "A novel affine arithmetic method to solve optimal power flow problems with uncertainties," *IEEE Trans. Power Syst.*, vol. 29, no. 6, pp. 2775–2783, Nov. 2014.
- [20] A. Gabash and P. Li, "Active-reactive optimal power flow in distribution networks with embedded generation and battery storage," *IEEE Trans. Power Syst.*, vol. 27, no. 4, pp. 2026–2035, Nov. 2012.
- [21] H. Kanchev, F. Colas, V. Lazarow, and B. Francois, "Emission reduction and economical optimization of an urban microgrid operation including dispatched PV-based active generators," *IEEE Trans. Sustain. Energy*, vol. 5, no. 4, pp. 1397–1405, Oct. 2014.
- [22] A. Sakti *et al.*, "Enhanced representations of lithium-ion batteries in power systems models and their effect on the valuation of energy arbitrage applications," *J. Power Sources*, vol. 342, pp. 279–291, 2017.
- [23] T. A. Nguyen and M. L. Crow, "Stochastic optimization of renewable-based microgrid operation incorporating battery operating cost," *IEEE Trans. Power Syst.*, vol. 31, no. 3, pp. 2289–2296, May 2016.
- [24] T. A. Nguyen, "Optimization in microgrid design and energy management," Doctoral Dissertations, Dept. Elect. Eng., Missouri University of Science and Technology, Rolla, Missouri, USA, 2014.
- [25] R. E. Rosenthal, "GAMS - A user's guide, GAMS development corporation," Washington, DC, USA, Dec. 2012.
- [26] B. Jiang and Y. Fei, "Smart home in smart microgrid: A cost-effective energy ecosystem with intelligent hierarchical agents," *IEEE Trans. Smart Grid*, vol. 6, no. 1, pp. 903–913, Jan. 2015.
- [27] M. Gulín, J. Matusko, and M. Vasak, "Stochastic model predictive control for optimal economic operation of a residential DC microgrid," in *Proc. IEEE Int. Conf. Ind. Technol.*, 2015, pp. 505–510.
- [28] P. Li, D. Xu, Z. Zhou, W. J. Lee, and B. Zhao, "Stochastic optimal operation of microgrid based on chaotic binary particle swarm optimization," *IEEE Trans. Smart Grid*, vol. 7, no. 1, pp. 66–73, Jan. 2016.
- [29] P. Fortenbacher, J. L. Mathieu, and G. Andersson, "Modeling and optimal operation of distributed battery storage in low voltage grids," *IEEE Trans. Power Syst.*, vol. 32, no. 6, pp. 4340–4350, Nov. 2017.
- [30] V. Mohan, J. G. Singh, and W. Ongsakul, "An efficient two stage stochastic optimal energy and reserve management in a microgrid," *Appl. Energy*, vol. 160, pp. 28–38, 2015.
- [31] K. Rahbar, J. Xu, and R. Zhang, "Real-time energy storage management for renewable integration in microgrid: An off-line optimization approach," *IEEE Trans. Smart Grid*, vol. 6, no. 1, pp. 124–134, Jan. 2015.
- [32] W. Ma, J. Wang, V. Gupta, and C. Chen, "Distributed energy management for networked microgrids using online ADMM with regret," *IEEE Trans. Smart Grid*, vol. 9, no. 2, pp. 847–856, Mar. 2018.

- [33] L. Yu, T. Jiang, and Y. Zhou, "Distributed real-time energy management in data center microgrids," *IEEE Trans. Smart Grid*, vol. 9, no. 4, pp. 3748–3762, Dec. 2016.
- [34] J. M. Nascimento and W. B. Powell, "An optimal approximate dynamic programming algorithm for the lagged asset acquisition problem," *Math. Operat. Res.*, vol. 34, no. 1, pp. 210–237, Feb. 2009.
- [35] A. Das and Z. Ni, "A computationally efficient optimization approach for battery systems in islanded microgrid," *IEEE Trans. Smart Grid*, to be published.
- [36] Z. Chen, L. Wu, and M. Shahidehpour, "Effective load carrying capability evaluation of renewable energy via stochastic long-term hourly based SCUC," *IEEE Trans. Sustain. Energy*, vol. 6, no. 1, pp. 188–197, Jan. 2015.
- [37] L. Zhang and Y. Li, "Optimal management for parking-lot electric vehicle charging by two-stage approximate dynamic programming," *IEEE Trans. Smart Grid*, vol. 8, no. 4, pp. 1722–1730, Jul. 2017.
- [38] C. Keerthisinghe, G. Verbic, and A. C. Chapman, "A fast technique for smart home management: ADP with temporal difference learning," *IEEE Trans. Smart Grid*, vol. 9, no. 4, pp. 3291–3303, Jul. 2018.
- [39] W. Powell, *Approximate Dynamic Programming: Solving the Curses of Dimensionality*. Hoboken, NJ, USA: Wiley, 2007.
- [40] Y. Shen, W. Yao, J. Y. Wen, and H. B. He, "Adaptive wide-area power oscillation damper design for photovoltaic plant considering delay compensation," *IET Gener., Trans. & Distrib.*, vol. 11, no. 18, pp. 4511–4519, Dec. 2017.
- [41] Y. Shen, W. Yao, J. Y. Wen, H. B. He, and W. B. Chen, "Adaptive supplementary damping control of VSC-HVDC for interarea oscillation using GrHDP," *IEEE Trans. Power Syst.*, vol. 33, no. 2, pp. 1777–1789, Mar. 2018.
- [42] D. R. Jiang and W. B. Powell, "Optimal hour-ahead bidding in the real-time electricity market with battery storage using approximate dynamic programming," *INFORMS J. Comput.*, vol. 27, no. 3, pp. 525–543, Aug. 2015.
- [43] H. Khorramdel, J. Aghaei, B. Khorramdel, and P. Siano, "Optimal battery sizing in microgrids using probabilistic unit commitment," *IEEE Trans. Ind. Inf.*, vol. 12, no. 2, pp. 834–843, Apr. 2016.



**Hang Shuai** (S'17) received the B.Eng. degree from Wuhan Institute of Technology, Wuhan, China, in 2013. He is currently working toward the Ph.D. degree in electrical engineering at the Huazhong University of Science and Technology, Wuhan, China.

His research interests include power systems operation and economics, stochastic optimization, and integrated energy system.



**Jiakun Fang** (S'10–M'13) received the B.Sc. and Ph.D. degrees from Huazhong University of Science and Technology, Wuhan, China, in 2007 and 2012, respectively.

He was with Huazhong University of Science and Technology, Wuhan, China. He is Currently an Assistant Professor with the Department of Energy Technology, Aalborg University, Aalborg, Denmark. His research interests include power system dynamic stability control, power grid complexity analysis, and integrated energy system.



**Xiaomeng Ai** (M'17) received the B.Eng degree in mathematics and applied mathematics and the Ph.D. degree in electrical engineering in 2008 and 2014, respectively, both from Huazhong University of Science and Technology (HUST), Wuhan, China.

He is Currently a Lecturer at HUST. His research interests include robust optimization theory in power system, renewable energy integration, and integrated energy market.



at HUST.

His current research interests include renewable energy integration, energy storage application, DC grid, and power system operation and control.

**Jinyu Wen** (M'10) received the B.Eng. and Ph.D. degrees all in electrical engineering from Huazhong University of Science and Technology (HUST), Wuhan, China, in 1992 and 1998, respectively. He was a visiting student from 1996 to 1997 and Research Fellow from 2002 to 2003, all from the University of Liverpool, U.K., and a Senior Visiting Researcher from the University of Texas at Arlington, USA, in 2010. From 1998 to 2002, he was the Director Engineer with XJ Electric Co. Ltd. in China. In 2003, he joined the HUST and now is a Professor



**Haibo He** (F'18) received the B.S. and M.S. degrees in electrical engineering from Huazhong University of Science and Technology, Wuhan, China, in 1999 and 2002, respectively, and the Ph.D. degree in electrical engineering from Ohio University, Athens, OH, USA, in 2006.

From 2006 to 2009, he was an Assistant Professor with the Department of Electrical and Computer Engineering, Stevens Institute of Technology. He is Currently the Robert Haas Endowed Chair Professor at the Department of Electrical, Computer, and Biomedical Engineering, the University of Rhode Island, Kingston, RI, USA. His research interests include smart grid, adaptive dynamic programming, computational intelligence, machine learning and data mining, and various applications.

He has authored and coauthored 1 sole-author research book (Wiley), edited 1 book (Wiley-IEEE) and 6 conference proceedings (Springer), and more than 300 peer-reviewed journal and conference papers. He served as the General Chair of the IEEE Symposium Series on Computational Intelligence (SSCI 2014). He was a recipient of the IEEE International Conference on Communications Best Paper Award (2014), the IEEE Computational Intelligence Society Outstanding Early Career Award (2014), National Science Foundation CAREER Award (2011), and Providence Business News Rising Star Innovator Award (2011). Currently, he is the Editor-in-Chief of the IEEE TRANSACTIONS ON NEURAL NETWORKS AND LEARNING SYSTEMS.